Determination of moment tensors from borehole data: a numerical analysis

Václav Vavryčuk

Geophysical Institute, Academy of Sciences of the Czech Republic, Boční II, 141 31 Praha 4, Czech Republic, E-mail: vv@ig.cas.cz

ABSTRACT

The complete moment tensors of seismic sources in homogeneous or vertically inhomogeneous isotropic structures cannot be retrieved using receivers deployed in one vertical borehole. The complete moment tensors can be retrieved from amplitudes of P waves, provided receivers are deployed in three boreholes at least. Using amplitudes of P and S waves, two boreholes are, in principle, sufficient. The similar rules apply also to transversely isotropic media with a vertical axis of symmetry.

In the case of limited observations, the inversion can be stabilized by imposing the zero-trace constraint on the moment tensors. However, this constraint is legitimate only if applied to observations of shear faulting on planar faults in isotropic media, which produces double-couple (DC) mechanisms. For shear faulting on non-planar faults, for tensile faulting, and for shear faulting in anisotropic media, the zero-trace constraint is no longer valid and can distort the retrieved moment tensor and bias the fault plane solution.

Numerical modelling simulating the inversion of the DC mechanism from real data reveals that the errors in the DC and non-DC percentages of the moment tensors rapidly decrease with increasing the number of boreholes used. For noisy P and S amplitudes with noise of 15% of the top amplitude at each channel and for a velocity model biased by 10%, the errors in the DC percentage attain 25, 13 and 6% when inverting for the DC mechanism from one, two and three boreholes.

1. INTRODUCTION

Careful monitoring of induced microseismicity of reservoirs helps in understanding the fracture process and enables the control of the rock fracturing to optimize reservoir production (Lumley 2001; Shoham 2001). The microseismic signals in reservoirs are commonly recorded by linear arrays of uniaxial or triaxial sensors deployed in wells. They are analyzed by detection algorithms, and the events are located to image fracturing as a function of time. Seismic waveforms are used to determine the source-time functions and moment tensors, which inform us about the size and orientation of fractures (Trifu and Shumila 2002; Rutledge *et al.* 1998; Nolen-Hoeksema and Ruff 2001; Rutledge and Phillips 2003). The moment tensors (MT) also inform us whether the fracture is opening or closing which is the key to monitoring the connectivity of the fracture (Ross *et al.* 1999; Maxwell and Urbancic 2001; Foulger *et al.* 2004).

The complete MT is described by six values and, in principle, can be determined from noise-free amplitudes of the P and S waves of the event observed at least at three stations. The raypaths of waves must have different directions and must not lie in a plane. In practice, the MT inversion is, however, more involved: the data are noisy, the stations are deployed in wells in linear arrays thus forming special configurations, and both the P and S waves are not always available in the recordings. In some cases this might invoke questions whether a particular experiment is properly designed and capable of inverting for the complete MT; and if not, how many MT components can be retrieved. In this paper, I analyze the impact of various sensor configurations on the retrieval of the moment tensors, and the limitations of the MT inversion due to inverting only selected types of waves. In numerical modeling, I show how robust the inversion is when using different borehole configurations and how biased the results are if we apply the zero-trace moment tensor condition which is commonly used for stabilizing the inversion (see Dufumier and Rivera 1997; Nolen-Hoeksema and Ruff 2001).

2. RADIATION FUNCTIONS IN ISOTROPIC AND ANISOTROPIC MEDIA

The wavefield generated by a point seismic source is expressed as follows (Aki and Richards 2002, Eq. 3.23):

$$u_i(\mathbf{x},t) = m_{kl} * G_{ik,l}\,, \tag{1}$$

where $u_i(\mathbf{x},t)$ is the displacement vector measured at point **x** and time *t*, $m_{kl}(t) = M_{kl} f(t)$ is the moment tensor function, M_{kl} is the seismic moment tensor, $f(t)$ is the source-time function, $G_{ik,l}$ is the spatial derivative of the Green function, and the symbol * stands for the time convolution. The moment tensor function describes the properties of the source, and the Green function describes the properties of the medium, in which the source is situated. Assuming that the medium is homogeneous and isotropic, and the receivers are far from the source (at least several wavelengths), we can express Eq. (1) as (Aki and Richards 2002, Eqs. 4.24, 4.25):

$$u_i(\mathbf{x},t) = \frac{R_i^P}{4\pi\rho\alpha^3}\frac{\dot{f}\left(t-\tau^P\right)}{r} + \frac{R_i^S}{4\pi\rho\beta^3}\frac{\dot{f}\left(t-\tau^S\right)}{r}\,, \tag{2}$$

where ρ is the density, α and β are the velocities of P and S waves, *r* is the distance from the source to the receiver, and τ^P and τ^S are the P- and S-wave travel times. Vectors $\mathbf{R}^P$ and $\mathbf{R}^S$ are the P- and S-wave radiation functions,

$$R_i^P = n_i n_k n_l M_{kl}\,, \tag{3}$$

$$R_i^S = -(n_i n_k - \delta_{ik}) n_l M_{kl}\,, \tag{4}$$

where vector **n** denotes the unit vector directed from the source to the receiver (the ray vector), and δ_{kl} is the Kronecker delta. The Einstein summation convention over repeated subscripts is applied. Assuming an isotropic moment tensor,

$$M_{kl} = M_0 \delta_{kl}\,, \tag{5}$$

equations (3) and (4) yield

$$R_i^P = M_0 n_i, \quad R_i^S = 0 \ . \tag{6}$$

Since the S-wave radiation function is zero in all directions, the source described by the isotropic moment tensor cannot be detected by measuring S waves.

Assuming that the medium is homogeneous and anisotropic, and the receivers are far from the source, we can express Eq. (1) as (Vavryčuk 2002, Eq. 10):

$$u_i(\mathbf{x},t) = \frac{1}{4\pi\rho} \frac{R_i^P}{v^P c^P \sqrt{K^P}} \frac{\dot{f}\left(t-\tau^P\right)}{r} + \frac{1}{4\pi\rho} \frac{R_i^{S1}}{v^{S1} c^{S1} \sqrt{K^{S1}}} \frac{\dot{f}\left(t-\tau^{S1}\right)}{r} + \frac{1}{4\pi\rho} \frac{R_i^{S2}}{v^{S2} c^{S2} \sqrt{K^{S2}}} \frac{\dot{f}\left(t-\tau^{S2}\right)}{r} \tag{7}$$

where v, c, K and τ are the group velocity, phase velocity, Gaussian curvature of the slowness surface and travel time, and the superscript denotes the type of wave (P, S1 or S2). The radiation function **R** for each wave is expressed as

$$R_i = g_i g_k s_l M_{kl}, \tag{8}$$

where vector **g** denotes the polarization vector of the wave, and **s** denotes the direction of the slowness vector. Vector **s** is generally different from the ray vector **n** calculated as the direction of the group velocity vector, $\mathbf{n} = \mathbf{v}/v$.

3. MOMENT TENSOR INVERSION IN ISOTROPIC MEDIA

3.1 One-borehole experiment

Let us consider an experiment with a vertical string of three-component (3-C) receivers placed in one vertical borehole. Let us fix the local coordinate system in such a way that the rays from the source to the receivers lie in the x_1-x_3 plane. Ray vector **n** is then expressed as $\mathbf{n} = (n_1, 0, n_3)^T$ and the P- and S-wave radiation functions of the source in an isotropic medium read

$$\mathbf{R}^P = \begin{bmatrix} n_1^3 M_{11} + 2n_1^2 n_3 M_{13} + n_1 n_3^2 M_{33} \\ 0 \\ n_1^2 n_3 M_{11} + 2n_1 n_3^2 M_{13} + n_3^3 M_{33} \end{bmatrix}, \tag{9}$$

$$\mathbf{R}^S = \begin{bmatrix} n_3^2 n_1 (M_{11} - M_{33}) + (n_3^2 - n_1^2) n_3 M_{13} \\ n_1 M_{12} + n_3 M_{23} \\ n_1^2 n_3 (M_{33} - M_{11}) + (n_1^2 - n_3^2) n_1 M_{13} \end{bmatrix}. \tag{10}$$

Equations (9) and (10) indicate that the P-wave radiation function does not depend on the MT components M_{12}, M_{22} and M_{23}, and the S-wave radiation function on the component M_{22}. Moreover, the S-wave radiation function is not sensitive to the trace of **M**, because it depends only on the difference $M_{11} - M_{33}$. This implies that data from a single borehole is insufficient to invert for the complete moment tensor. When inverting P waves, we can get three components of the moment tensor: M_{11}, M_{33} and M_{13}. When inverting S waves, we can get three components of the moment tensor: M_{12}, M_{13}, M_{23}, and the difference $M_{11} - M_{33}$. Inverting P and S waves simultaneously yields five components of the moment tensor. The unrecoverable component of **M** is M_{22}. This result has been derived for homogeneous isotropic media, but it obviously applies also to horizontally layered media or to inhomogeneous media with a vertical gradient. The impossibility of recovering the complete moment tensor from a single borehole has been recognized by Nolen-Hoeksema and Ruff (2001).

3.2 Multi-borehole experiment

Let us consider an experiment with a vertical string of 3-C receivers placed in several vertical boreholes. Let us define the local coordinate system in such a way that the rays from the source to the receivers in the first borehole lie in the x_1-x_3 plane. Obviously, data from additional boreholes improve the conditionality of the moment tensor equations. Inserting direction vectors **n** into (3) for receivers in all boreholes, we obtain a set of equations for the moment tensor. Depending on the number of boreholes used, we are able to determine a different number of moment tensor components (see Tables 1 and 2).

For determining the complete MT we have to measure amplitudes of P waves from at least three boreholes, or amplitudes of P and S waves from two boreholes. Utilizing amplitudes of S waves, the complete MT cannot be retrieved from any number of boreholes, since S waves are not sensitive to the trace of the moment tensor.

Table 1. Number of components of **M** recoverable in isotropic media

Waves	1 well	2 wells	3 wells or more
P	3	5	6
S	4	5	5
P+S	5	6	6

Table 2. Components of **M** unrecoverable in isotropic media

Waves	1 well	2 wells	3 wells or more
P	M_{12}, M_{22}, M_{23}	M_{12}/M_{22}	-
S	Tr(**M**), M_{22}	Tr(**M**)	Tr(**M**)
P+S	M_{22}	-	-

The moment tensor components are specified in the local coordinate system, in which the first borehole is along the x_3-axis and the rays lie in the x_1-x_3 plane.

4. MOMENT TENSOR INVERSION IN ANISOTROPIC MEDIA

In this section, I shall shortly discuss basic differences between the MT inversion in isotropy and in general anisotropy. After that I shall focus on the MT inversion in transverse isotropy with a vertical axis of symmetry that is the most frequent anisotropy in exploration seismic.

4.1 One-borehole experiment in triclinic anisotropy

Let us consider a one-borehole experiment situated in a medium with triclinic anisotropy. Let us define the local coordinate system to observe the rays from the source to the receivers in the x_1-x_3 plane. Ray vector **n** is then expressed as $\mathbf{n} = (n_1, 0, n_3)^T$ and the

radiation functions of a seismic source are expressed by Eq. (8). Since the slowness and polarization vectors in anisotropic media have directions $\mathbf{g}=(g_1,g_2,g_3)^T$, $\mathbf{s}=(s_1,s_2,s_3)^T$, which need not be parallel or perpendicular to the ray vector, the radiation functions depend on all components of the moment tensors. Consequently, one-borehole data can be used, in principle, for inverting for the complete moment tensor. However, from practical viewpoint, this task is unfeasible for several reasons. First, we usually do not have an accurate and complete knowledge of triclinic anisotropy. Second, in majority of geophysically interesting cases anisotropy displays some symmetry. This causes that the radiation functions need not depend on all MT components, similarly as in isotropic media, and therefore the complete MT cannot be retrieved. Third, anisotropy is usually weak and the medium is inhomogeneous, which causes that the inversion for the complete MT becomes unstable.

4.2. One- and multi-borehole experiments in transverse isotropy

Now, let us consider the transversely isotropic medium with a vertical axis of symmetry (VTI). In this case, the seismic source generates P, SV and SH waves with the following polarization vectors and the directions of the slowness vectors:

$$\mathbf{g}^P=\begin{bmatrix} g_1^P \\ 0 \\ g_3^P \end{bmatrix},\ \mathbf{g}^{SV}=\begin{bmatrix} g_1^{SV} \\ 0 \\ g_3^{SV} \end{bmatrix},\ \mathbf{g}^{SH}=\begin{bmatrix} 0 \\ 1 \\ 0 \end{bmatrix},$$

$$\mathbf{s}^P=\begin{bmatrix} s_1^P \\ 0 \\ s_3^P \end{bmatrix},\ \mathbf{s}^{SV}=\begin{bmatrix} s_1^{SV} \\ 0 \\ s_3^{SV} \end{bmatrix},\ \mathbf{s}^{SH}=\begin{bmatrix} s_1^{SH} \\ 0 \\ s_3^{SH} \end{bmatrix}. \tag{11}$$

The radiation functions are expressed as follows:

$$\mathbf{R}^W=\begin{bmatrix} (g_1^W)^2 s_1^W M_{11}+g_1^W\left(g_1^W s_3^W+g_3^W s_1^W\right)M_{13}+g_1^W g_3^W s_3^W M_{33} \\ 0 \\ g_1^W g_3^W s_1^W M_{11}+g_3^W\left(g_1^W s_3^W+g_3^W s_1^W\right)M_{13}+(g_3^W)^2 s_3^W M_{33} \end{bmatrix}, \tag{12}$$

$$\mathbf{R}^{SH} = \begin{bmatrix} 0 \\ s_1^{SH} M_{12} + s_3^{SH} M_{23} \\ 0 \end{bmatrix}, \tag{13}$$

where W stands for P or SV.

Equations (12) and (13) indicate that the P- and SV-wave radiation functions do not depend on the MT components M_{12}, M_{22} and M_{23}, and the SH-wave radiation function on the components M_{11}, M_{22}, M_{33} and M_{13}. Hence, when inverting the P or SV waves gathered at one borehole, we can get three MT components, and when inverting the SH waves, we can get two MT components (see Tab. 3). Inverting the P, SV and SH waves simultaneously yields five components of the moment tensor. Similarly as for isotropic media, we cannot recover the M_{22} component using the data gathered by one vertical borehole (see Tab. 4). This result is valid also for other symmetries of anisotropy such as orthorhombic anisotropy, provided the seismic source and the borehole lie in the symmetry plane.

In the case of the two-borehole experiment, we can determine 5 components of the moment tensor when inverting P or SV waves, and we can determine 3 components of the moment tensor when inverting SH waves. If we combine SV and SH waves, or P, SV and SH waves, then the complete moment tensor can be determined.

Table 3. Number of components of **M** recoverable in VTI

Waves	1 well	2 wells	3 wells or more
P	3	5	6
SV	3	5	6
SH	2	3	3
SV+SH	5	6	6
P+SV+SH	5	6	6

Table 4. Components of **M** unrecoverable in VTI

Waves	1 well	2 wells	3 wells or more
P	M_{12}, M_{22}, M_{23}	M_{12}/M_{22}	-
SV	M_{12}, M_{22}, M_{23}	M_{12}/M_{22}	-
SH	M_{11}, M_{22}, M_{33}, M_{13}	M_{11}, M_{22}, M_{33}	M_{11}, M_{22}, M_{33}
SV+SH	M_{22}	-	-
P+SV+SH	M_{22}	-	-

The moment tensor components are specified in the local coordinate system, in which the first borehole is along the x_3-axis and rays lie in the x_1-x_3 plane.

5. NUMERICAL MODELING

In this section, I shall focus on estimating errors produced by the moment tensor inversion of amplitudes of P and S waves observed at one, two or three boreholes located in an isotropic medium. To mimic conditions of real experiments, I shall assume in the MT inversion: (1) an inaccurate knowledge of the medium, (2) a mislocated source, and (3) noisy amplitudes of waves. Moreover, the inversion will be performed under the assumption that the moment tensors have a zero trace. This condition is necessary to apply to the one-borehole experiment, where only five components of the moment tensors can be inverted (see Tab. 1), so the inversion must be stabilized (see Nolen-Hoeksema and Ruff 2001). Applying this condition in multi-borehole experiments is not necessary, but still frequently adopted in practice. Here I shall show how the results can be distorted if the source is not shear and the true moment tensor has a non-zero trace.

5.1. Geometry of the experiment

Let us assume a seismic source located at depth of 1.5 km. The three vertical observation boreholes are positioned at distance of 0.5 km from the source in azimuths of 90º (borehole 1), 60º (borehole 2) and 30º (borehole 3). Each borehole is equipped by 11 three-component receivers deployed at depths from 0.5 to 1.5 km with step of 100 m. The medium is homogeneous and isotropic with P and S velocities, v^P=4.0 km/s and v^S=2.5 km/s, respectively.

The seismic source is defined by the orientation of the fault plane and by the slip vector (see Vavryčuk 2001, eq. 1). The fault plane is vertical and characterized by a strike of 0º. The slip lies in the horizontal plane and its azimuth varies from 0º to 180º. Hence the studied sources cover all possible combinations from the pure shear source (see Fig. 1a, the slip azimuth is 0º and 180º) to the pure tensile source (the slip azimuth is 90º). Physically, the tensile sources correspond to opening of faults or fractures during the hydrofracture experiments (see Fig. 1b)

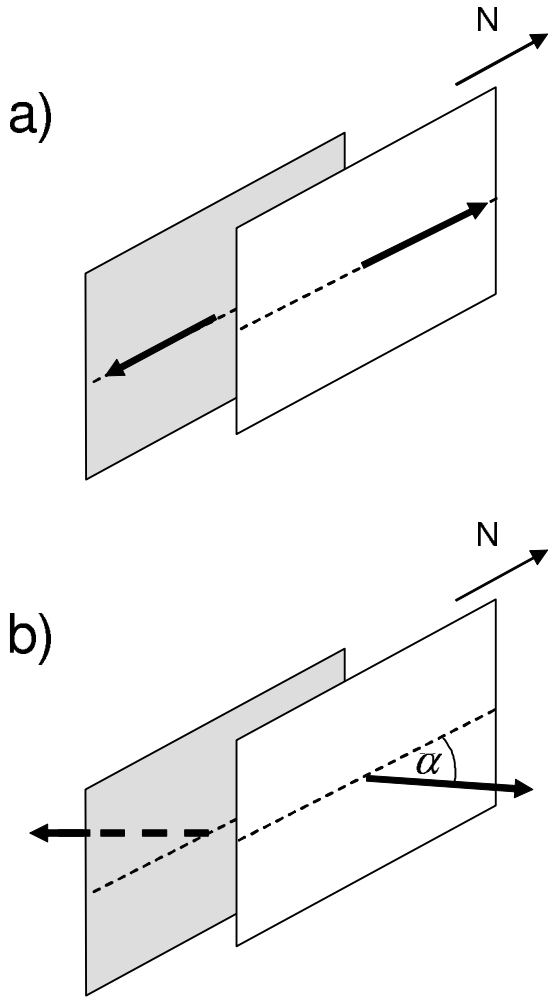

Figure 1. Geometry of faulting: shear faulting (a), tensile faulting (b). The fault is vertical in the N-S direction, the slip lies in the horizontal plane.

Since the sources under study are generally non-shear, the moment tensors contain the double-couple (DC) part as well as the non-double-couple (non-DC) part (see Vavryčuk, 2001). The non-DC part consists of the compensated linear vector dipole (CLVD) component and the isotropic (ISO) component. The percentages of the ISO and CLVD depend on the orientation of the slip with respect to the fault normal (see Fig. 2). If the slip lies in the fault plane (the slip azimuth is 0° or 180°), the source is pure shear and contains no non-DC components. For the other directions, the source is partly tensile and the non-DC components are non-zero. For pure tensile source (the slip azimuth is 90°), the DC is zero, and the ISO and CLVD are positive and attain their maximum values.

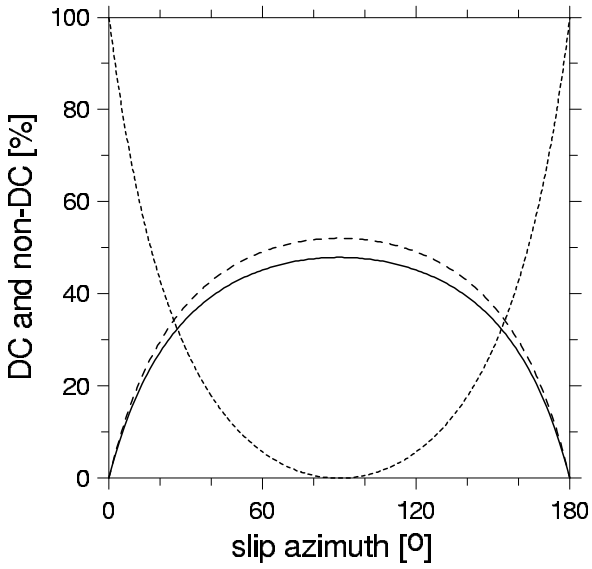

Figure 2. The DC and non-DC components of the moment tensor. The percentages of the ISO (solid line), CLVD (dashed line), and DC (dotted line) components are shown as a function of the slip azimuth. The value of the azimuth coincides with the deviation of the slip from the fault plane. The percentages of the DC and non-DC components were calculated using formulas (8a-c) of Vavryčuk (2001).

5.2. Inversion scheme

In the next numerical tests, the MT inversion from far-field amplitudes of P and S waves will be used. The amplitudes A_i observed at one three-component sensor are expressed as follows:

$$A_i^W = M_{kl} G_{ik,l}^W , \tag{14}$$

where W stands for P or S, and $G_{ik,l}^P$ and $G_{ik,l}^S$ are defined as

$$G_{ik.l}^P = \frac{n_i n_k n_l}{4\pi\rho\alpha^3 r} , \quad G_{ik.l}^S = -\frac{(n_i n_k - \delta_{ik}) n_l}{4\pi\rho\beta^3 r} . \tag{15}$$

Observing amplitudes at many sensors, equation (14) can be used to form a system of linear equations for unknown MT components M_{kl}. The optimum MT is then solved by minimizing the sum of differences between the theoretical and observed amplitudes in the least-square sense.

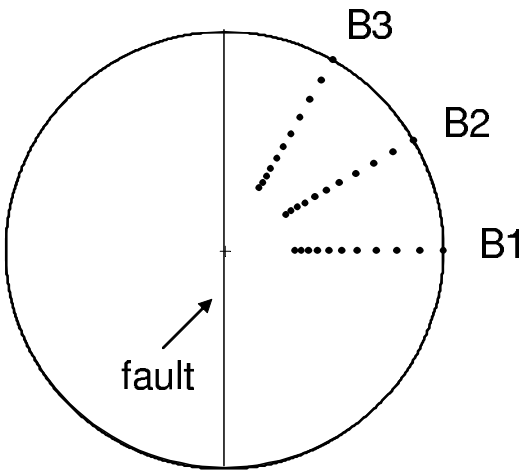

Figure 3. The configuration of the experiment in the upper-hemisphere equal-area projection. B1, B2 and B3 denote the boreholes, dots mark the positions of the sensors. The plus sign marks the position of the source. The straight line shows the projection of the fault.

5.3. Inversion from noise-free amplitudes

First, I shall assume that the observed amplitudes are noise-free. I shall compare results of the MT inversion performed under the assumptions of an exact and approximate knowledge of the medium and of the accurately located and mislocated source. The approximate model of the medium will be biased from the exact model by 10% being characterized by the P- and S-wave velocities of 4.4 and 2.75 km/s. The approximate directions of rays from the source to the receivers will be shifted due to the mislocation of the source by 10° in azimuth..

For the above described geometry of faulting and the borehole configuration (see Fig. 3), I calculated the true MT of the source using eq. (1) of Vavryčuk (2001), and theoretical amplitudes of P and S waves radiated from the source and recorded by borehole sensors using eqs (14-15). Then I inverted the amplitudes for the complete MT using exact and approximate Green's functions. I performed three numerical experiments by inverting the data from boreholes: (a) B1, (b) B1 and B2, and (c) B1, B2 and B3. The retrieved moment tensors were constraint to have zero trace, which is equivalent to zero ISO components.

Figure 4 shows the errors of the CLVD and DC percentages of the source, and the errors in the strike of the fault calculated when inverting with the exact medium model and with the exact source location. The figures indicate that all inversions were successful for pure shear sources: for the slip azimuths of 0° and 180°, the inversions yield correct values of the CLVD and DC, and also the retrieved orientation of the fault is correct. However, the results are less accurate for the other directions. For the one-borehole experiment, the errors of the CLVD and DC attain values up to 80% and 60%, respectively. For multi-borehole experiments, the errors of the CLVD attain values up to 40%. The errors in the DC decrease with an increasing number of boreholes, being about 15% for the three-borehole experiment. Also the retrieved strike of the fault is erroneous. The errors can attain values up to 45° and their dependence on the slip azimuth is roughly the same for all experiments.

The maximum errors in the strike of the fault and in the percentages of the DC and CLVD are produced when the pure tensile source is inverted (the slip azimuth is 90°). This is caused by the assumption of the zero-trace moment tensors, which is completely inconsistent with the pure tensile source. Of course, if we do not apply the zero-trace constraint then we obtain the correct strike of the fault as well as correct percentages of the

DC, CLVD and ISO components. However, this is possible only in multi-borehole experiments, because they are robust enough to invert for the complete MT without applying any a priori constraint.

Figure 5 shows the errors of the CLVD and DC percentages of the source, and the errors of the strike of the fault, when inverting with an approximate medium model and with a mislocated source. In this case, the inversion yields inaccurate values of the DC, CLVD and strike even for pure shear sources (slip azimuths of 0° and 180°). For the one-borehole experiment, the DC and CLVD error is about 20%. For the two- and three-borehole experiments the error decreases to 12% and 5%, respectively. The error of the strike is roughly 10° for all experiments and is produced by the mislocation of the source. For tensile sources, the errors of the DC, CLVD and strike increase to similar values produced when inverting for MT with exactly modeled medium and with the exact source location. This indicates that a wrong assumption imposed on the source (the zero ISO component) distorts the results more seriously than the application of the inaccurate medium model or the mislocated source.

5.4. Inversion from noisy amplitudes

Similar numerical experiments as in Sec. 5.3 have been performed also for noisy data. The noisy P and S amplitudes were generated from the true P and S amplitudes by adding a noise with a uniform distribution and with maximum amplitude reaching ±15% of the top amplitude at each channel. In order to obtain statistically relevant results, we performed one hundred MT inversions, each of them with a different noise realization. In the MT inversions, we consider the approximate medium model and the mislocated source as in Sec 5.3. We assumed two types of the source: a pure DC source (with slip azimuth of 0°) and a tensile source (with slip azimuth of 60°). The moment tensors were constrained to have the zero trace.

Figure 6 shows the histograms of the CLVD, DC and strike errors for the shear event. The most frequent error in the CLVD and DC percentages is about 24% for one-borehole experiment. For two- and three-borehole experiments, the error decreases to 13% and 6%, respectively. Hence as expected, the one-borehole experiment is most vulnerable to errors in amplitudes, and to mismodelling of the medium. The error in the strike is about 10° for all experiments and is due to the mislocation of the source.

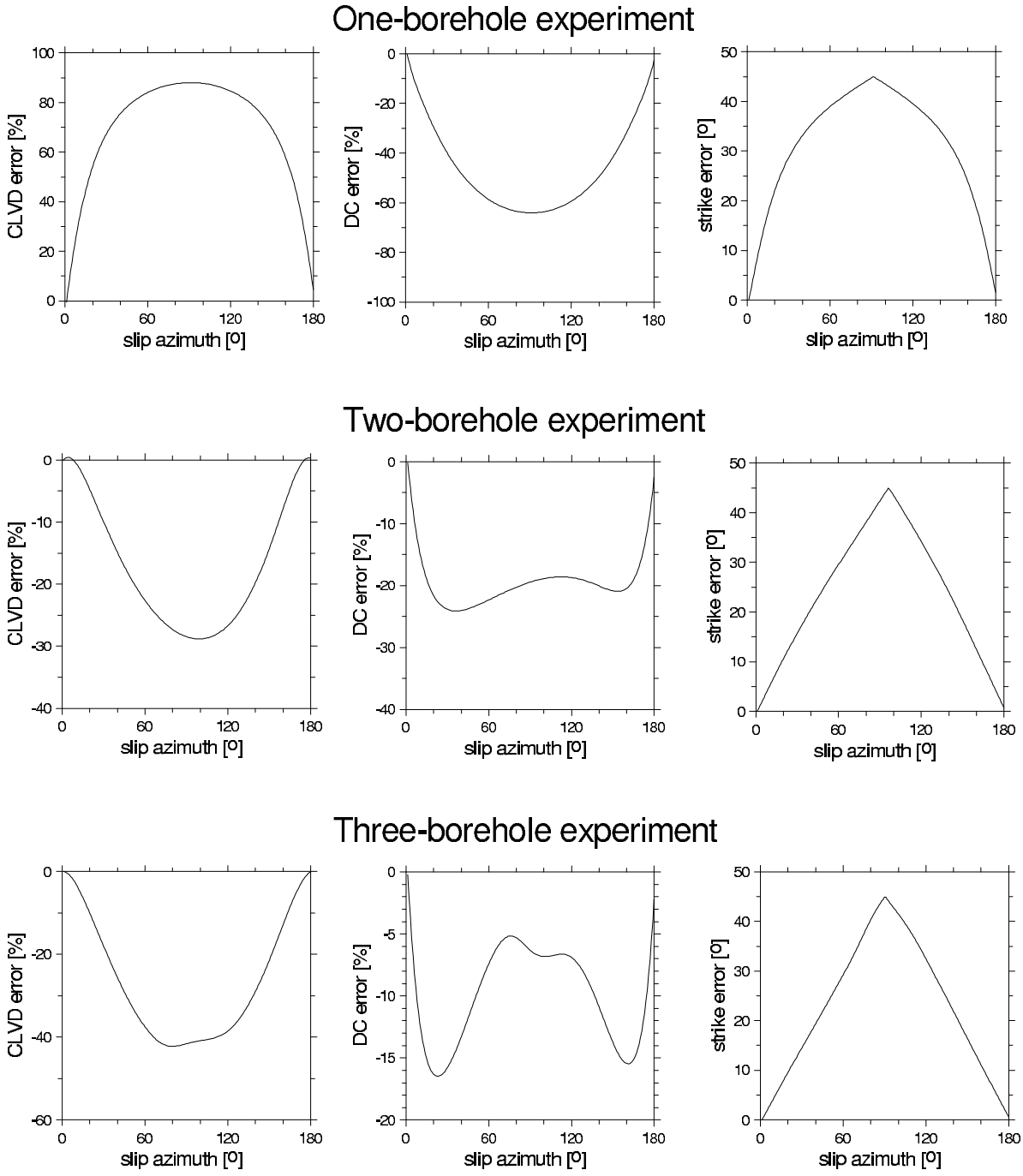

Figure 4. The errors of the CLVD, DC and strike as a function of the slip direction for the one-borehole, two-borehole, and three-borehole experiments. The errors are calculated as the difference between the exact and calculated values. The inversion is performed using the exact medium model and the accurate location of the source.

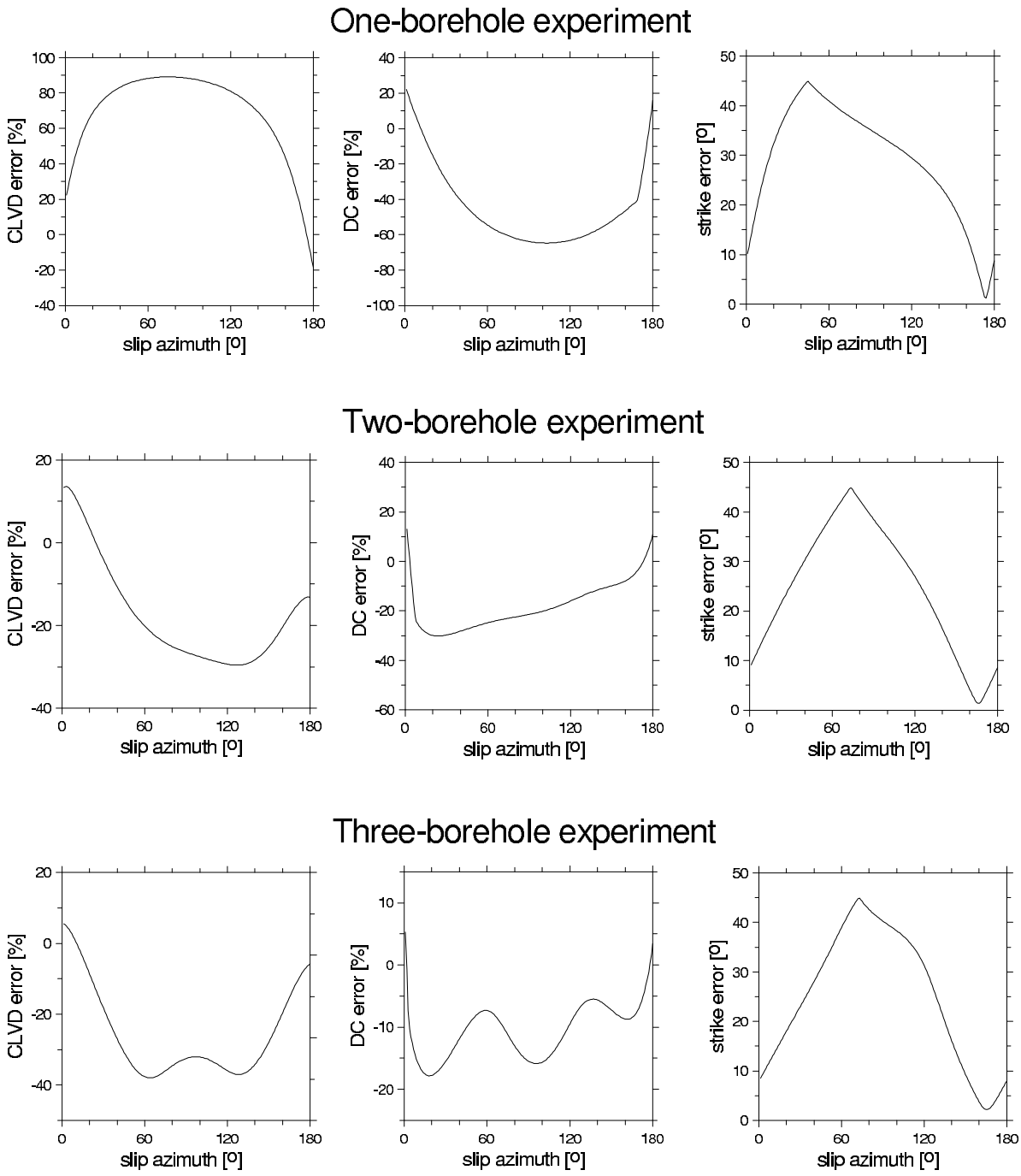

Figure 5. The errors of the CLVD, DC and strike as a function of the slip direction for the one-borehole, two-borehole, and three-borehole experiments. The errors are calculated as the difference between the exact and calculated values. The inversion is performed using the approximate medium model and the mislocated source.

Figure 7 shows the histograms of the CLVD, DC and strike errors for the tensile event with the slip azimuth of 60°. In this case, the MT inversion totally fails for the one-borehole experiment. The two- and three-borehole experiments also fail in estimating the strike of the fault and the CLVD percentage. The estimation of the DC percentage is, however, better: the three-borehole experiment yields the most frequent error in the DC percentage of 6% only. This value is in agreement with the results obtained by the MT inversion from noise-free data. This indicates that random noise is not the primary factor deteriorating the accuracy of the results. The primary origin of errors of the MT inversion in the multi-borehole experiments is the zero-trace constraint.

6. CONCLUSIONS

It is not possible to retrieve the complete MT of seismic sources in a homogeneous isotropic structure from data gathered by receivers deployed in one vertical (or straight inclined) borehole. Three MT components can be retrieved using amplitudes of P waves, four components using amplitudes of S waves, and five components using amplitudes of both the P and S waves. The complete MT can be retrieved from amplitudes of P waves, provided that receivers are deployed in three parallel boreholes or at least in two non-parallel boreholes. The boreholes must be in different azimuths from the source. Using the amplitudes of P and S waves, two (either parallel or non-parallel) boreholes are, in principle, sufficient to retrieve the complete MT. Using amplitudes of the S waves only, we can never determine the trace of the moment tensor regardless of the number of boreholes used.

The above conclusions also apply to layered isotropic structures or to isotropic structures with a velocity gradient, provided the normal to the layers or the gradient direction is along the direction of the borehole. If the medium is transversely isotropic with the symmetry axis parallel to the borehole, the moment tensors can be retrieved under conditions similar to those valid for isotropic media. The only difference is that the SV and SH waves in TI media contain slightly more information than the S waves in isotropic media. For example, we can invert for the complete MT using the amplitudes of the SV and SH waves in TI gathered at least at two boreholes (see Tab. 3), while we can never do this using the amplitudes of the S waves in isotropy (see Tab. 1).

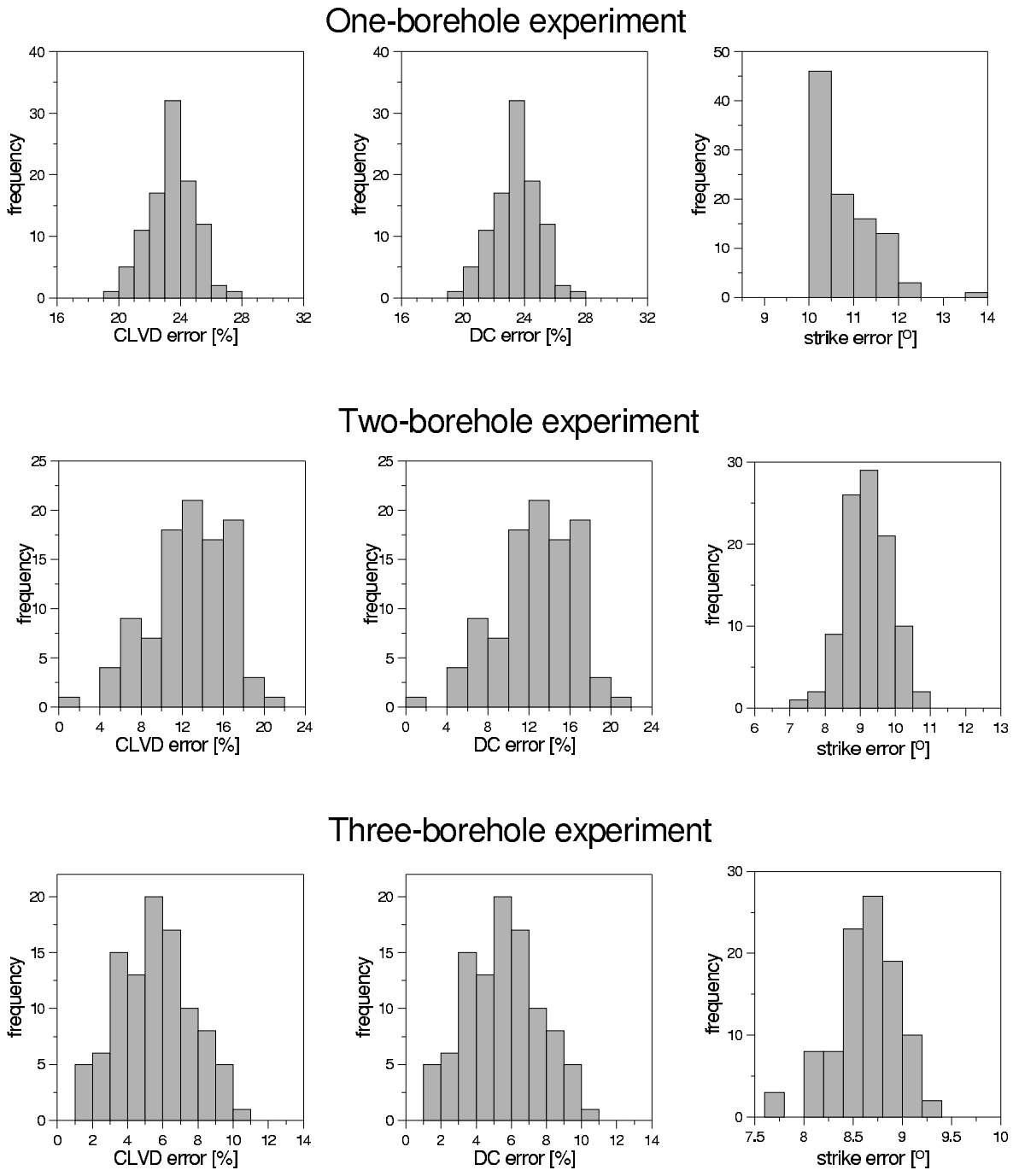

Figure 6. The histograms of errors of the CLVD, DC and strike. The true moment tensor is pure DC. The inversion is performed from noisy amplitudes and using the approximate medium model and the mislocated source.

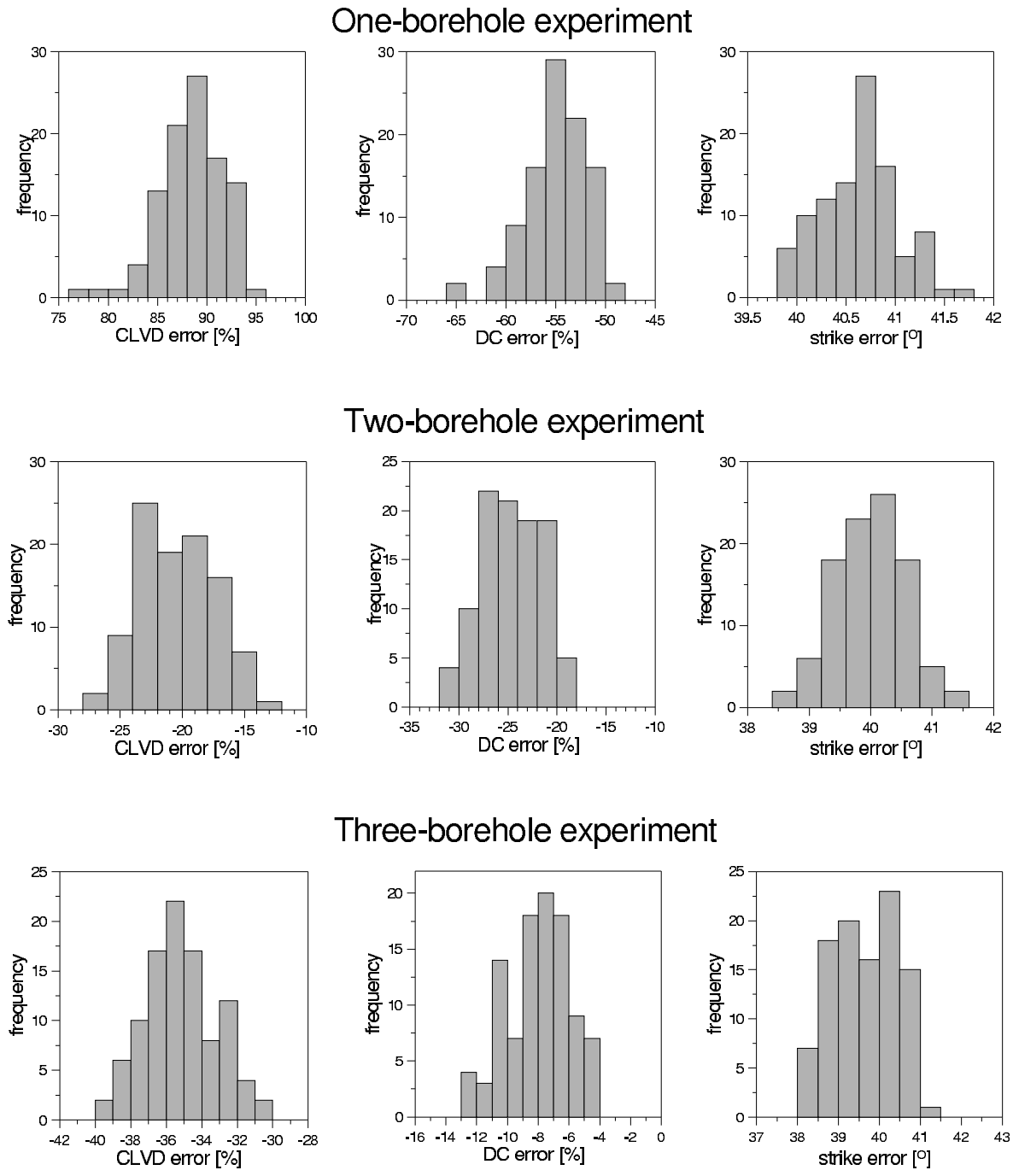

Figure 7. The histograms of errors of the CLVD, DC and strike. The true moment tensor is non-DC (the slip azimuth is 60°). The inversion is performed from noisy amplitudes and using the approximate medium model and the mislocated source.

If the geometry of the experiment prevents retrieving the complete MT, the inversion can be stabilized by imposing the condition of zero trace of the moment tensor. This works for inverting from the P and S amplitudes measured in one borehole, from the P amplitudes measured in two boreholes, or from the S amplitudes measured in two or more boreholes. The zero-trace condition, however, may be legitimately applied only to observations of shear faulting on planar faults in isotropic media, which produces double-couple mechanisms. If the source area is anisotropic (see Rössler *et al.* 2004; Vavryčuk 2005a,b) or if the source is more complex, containing a non-zero tensile component (see Vavryčuk 2001), the zero-trace condition is no longer valid. In this case, the source produces a general non-double-couple mechanism (Frohlich 1994; Julian *et al.* 1998; Miller *et al.* 1998) and applying the zero-trace constraint can distort the retrieved moment tensor and bias the fault plane solution. The numerical modeling shows that when inverting tensile sources under the zero-trace constraint, the DC component can be significantly overestimated and the retrieved CLVD can have even a wrong sign. The bias in the fault orientation is proportional to the amount of the tensile component in the source and can attain values up to 45° for pure tensile faulting. Obviously, to eliminate these errors, the moment tensors must be inverted without any constraint and the experiments must be designed to be sufficiently robust for doing this job. This can be achieved by an experiment with two monitoring boreholes at least and by processing both P and S waves. Optimally, the inversion for the complete MT should be supplemented by estimates of their reliability and by the error analysis (Šílený 1998; Trifu *et al.* 2000; Trifu and Shumila 2002; Šílený 2004).

ACKNOWLEDGEMENTS

I thank Leo Eisner, Luděk Klimeš and two anonymous reviewers for their comments, and Susanne Rentsch for drawing my attention to the problem under study. This work was supported by the Grant Agency of the Academy of Sciences of the Czech Republic, Grants No. IAA3012309 and IAA300120502, by the Consortium Project SW3D "Seismic waves in complex 3-D structures", and by the EU Consortium Project IMAGES "Induced microseismics applications from global earthquake studies", Contract No. MTKI-CT-2004-517242. A part of the work was done while the author was a visiting researcher at the Schlumberger Cambridge Research, Cambridge, U.K.

REFERENCES

Aki K. and Richards P.G. 2002. *Quantitative Seismology*. University Science Books, Sausalito, California.

Dufumier H. and Rivera L. 1997. On the resolution of the isotropic component in moment tensor inversion. *Geophys. J. Int.* **131**, 595-606.

Foulger G.R., Julian B.R., Hill D.P., Pitt A.M., Malin P.E. and Shalev E. 2004. Non-double-couple microearthquakes at Long Valley caldera, California, provide evidence for hydraulic fracturing. *J. Volcan. Geotherm. Res.* **132**, 45-71.

Frohlich C. 1994. Earthquakes with non-double-couple mechanisms. *Science* **264**, 804-809.

Julian B.R., Miller A.D., and Foulger G.R. 1998. Non-double-couple earthquakes, 1. Theory. *Rev. Geophys.* **36**, 525-549.

Lumley D.E. 2001. The next wave in reservoir monitoring: The instrumented oil field. *Leading Edge* **20**, 640-648.

Maxwell S.C. and Urbancic T.I. 2001. The role of passive microseismic monitoring in the instrumented oil field. *Leading Edge* **20**, 636-640.

Miller A.D., Foulger G.R., and Julian B.R. 1998. Non-double-couple earthquakes, 2. Observations. *Rev. Geophys.* **36**, 551-568.

Nolen-Hoeksema R.C. and Ruff L.J. 2001. Moment tensor inversion of microseisms from the B-sand propped hydrofracture, M-site, Colorado. *Tectonophysics* **336**, 163-181.

Rössler D., Rümpker G., and Krüger F. 2004. Ambiguous moment tensors and radiation patterns in anisotropic media with applications to the modeling of earthquake mechanisms in W-Bohemia. *Stud. Geophys. Geod.* **48**, 233-250.

Ross A., Foulger G.R., and Julian B.R. 1999. Source processes of industrially-induced earthquakes at The Geysers geothermal area, California. *Geophysics* **64**, 1877-1889.

Rutledge J.T. and Phillips W.S. 2003. Hydraulic stimulation of natural fractures as revealed by induced microearthquakes, Carthage Cotton Valley gas field, east Texas. *Geophysics* **68**, 441-452.

Rutledge J.T., Phillips W.S. and Schuessler B.K. 1998. Reservoir characterization using oil-production-induced microseismicity, Clinton County, Kentucky. *Tectonophysics* **289**, 129-152.

Shoham Y. 2001. Future oil fields and what subsurface technologists will need to know. *Leading Edge* **20**, 572.

Šílený J. 1998. Earthquake source parameters and their confidence regions by a genetic algorithm with a 'memory'. *Geophys. J. Int.* **134**, 228-242.

Šílený J., 2004. Regional moment tensor uncertainty due to mismodeling of the crust. *Tectonophysics* **383**, 133-147.

Trifu C-I., Angus D. and Shumila V. 2000. A fast evaluation of the seismic moment tensor for induced seismicity. *Bull. Seism. Soc. Am.* **90**, 1521-1527.

Trifu C-I. and Shumila V. 2002. Reliability of seismic moment tensor inversions for induced microseismicity at Kidd Mine, Ontario. *Pure Appl. Geophys.* **159**, 145-164.

Vavryčuk V. 2001. Inversion for parameters of tensile earthquakes. *J. Geophys. Res.* **106**, No. B8, 16.339-16.355.

Vavryčuk V. 2002. Asymptotic elastodynamic Green function in the kiss singularity in homogeneous anisotropic solids. *Stud. Geophys. Geod.* **46**, 249-266.

Vavryčuk V. 2005a. Focal mechanisms in anisotropic media. *Geophys. J. Int.* **161**, 334-346, doi: 10.1111/j.1365-246X.2005.02585.x.

Vavryčuk V. 2005b. Focal mechanisms produced by shear faulting in weakly transversely isotropic crustal rocks. *Geophysics*, in print.